



Deposited via The University of Sheffield.

White Rose Research Online URL for this paper:

<https://eprints.whiterose.ac.uk/id/eprint/74665/>

---

**Monograph:**

Zhao, Y., Billings, S.A., Coca, D. et al. (2010) Identification of a temperature dependent FitzHugh-Nagumo model for the Belousov-Zhabotinskii reaction. Research Report. ACSE Research Report no. 1014 . Automatic Control and Systems Engineering, University of Sheffield

---

**Reuse**

Items deposited in White Rose Research Online are protected by copyright, with all rights reserved unless indicated otherwise. They may be downloaded and/or printed for private study, or other acts as permitted by national copyright laws. The publisher or other rights holders may allow further reproduction and re-use of the full text version. This is indicated by the licence information on the White Rose Research Online record for the item.

**Takedown**

If you consider content in White Rose Research Online to be in breach of UK law, please notify us by emailing [eprints@whiterose.ac.uk](mailto:eprints@whiterose.ac.uk) including the URL of the record and the reason for the withdrawal request.

# Identification of a Temperature Dependent FitzHugh-Nagumo model for the Belousov-Zhabotinskii Reaction

Y. Zhao, S.A. Billings, D.Coca , Y.Guo, R.I.Ristic, L.L.De Matos



Research Report No. 1014

Department of Automatic Control and Systems Engineering  
The University of Sheffield  
Mappin Street, Sheffield,  
S1 3JD, UK

September, 2010

# Identification of a Temperature Dependent FitzHugh-Nagumo model for the Belousov-Zhabotinskii Reaction

Y.Zhao, S.A.Billings, D.Coca, Y.Guo \*; R.I.Ristic, L.L.DeMatos †

September 16, 2010

## Abstract

This paper describes the identification of a temperature dependent FitzHugh-Nagumo model directly from experimental observations with controlled inputs. By studying the steady states and the trajectory of the phase of the variables, the stability of the model is analysed and a rule to generate oscillation waves is proposed. The dependence of the oscillation frequency and propagation speed on the model parameters is then investigated to seek the appropriate control variables, which then become functions of temperature in the identified model. The results show that the proposed approach can provide a good representation of the dynamics of the oscillatory behaviour of a BZ reaction.

## 1 Introduction

The Belousov-Zhabotinskii (BZ) chemical reaction has been well established as a prototype system for studies of reaction-diffusion phenomena and pattern formation. Many models have been developed to describe the rich properties including exhibiting interesting temporal oscillations and spatial patterns [FitzHugh, 1955; Glansdorff and Prigogine, 1971; Field and Noyes, 1974; Gray and Scott, 1983; Chou et al., 2007]. Recently, more

---

\*Department of Automatic Control and System Engineering, University of Sheffield, UK.

†Department of Chemical and Process Engineering, University of Sheffield, UK.

investigators have studied the identification of models of the BZ reaction directly from experimental data. A Cellular Automata (CA) model was presented in [Zhao et al., 2007] to describe the propagation behaviour in a BZ reaction where the value of the brightness of each pixel was limited to finite states. Guo [Guo et al., 2010] introduced a Coupled Map Lattice (CML) model, where the diffusion and reaction parts were separated. A revised FitzHugh-Nagumo (R-FHN) model was proposed in [Zhao et al., 2010] by establishing the dependence of the wave profile and propagation speed on the model parameters. These identified models can describe a rich variety of BZ patterns such as spiral waves, oscillating waves or Turing patterns etc. However, very little attention has been paid to identify the observations of a BZ reaction with controlled inputs, which can be light [Kaminaga et al., 2006], temperature [Ito et al., 2003; Vanag and Epstein, 2008], initial concentration of the ingredients [Bansagi et al., 2009] or manual interference [Adamatzkya et al., 2004]. It is very important to be able to identify a mathematical model directly from experimental data where the parameters or terms are functions of the controllable physical variables. By utilizing such a model, specific behaviours of real spatio-temporal systems can be designed by controlling the model parameters. This also helps in predicting patterns which exist under extreme physical conditions and which may be difficult to reproduce in the laboratory, which could be highly attractive in several applications.

Temperature is one vital parameter that has a significant influence on the dynamics of the chemical oscillations [Zhabotinskii, 1964; Koros, 1974] in the BZ reaction. Recently, from the chemical point of view, [Pullela et al., 2009] presented a five-step temperature dependent Oregonator model to describe the BZ reaction, but this study was only focused on simulations in theory. By investigating a variety of observations over changing temperature from  $20^{\circ}C$  to  $45^{\circ}C$  in the BZ reaction, this paper describes the identification of a temperature dependent FitzHugh-Nagumo (TD-FHN) model from real experimental data, in terms of the chemical oscillation frequency and propagation speed.

The paper is organized as follows. A TD-FHN model is presented in Section 2 together with an associated stability analysis. Section 3 introduces the routine to identify the parameters of the model based on experimental data. Finally, the conclusions are given in Section 4.

## 2 Temperature Dependent FitzHugh-Nagumo Model

A traditional FitzHugh-Nagumo model(FHN) can be expressed as:

$$\begin{aligned}\frac{\partial u}{\partial t} &= f(u, v) = u(a - u)(u - 1) - v + \nabla^2 u \\ \frac{\partial v}{\partial t} &= g(u, v) = bu - \gamma v\end{aligned}\tag{1}$$

where  $u, v$  are two variables;  $f(u, v)$  and  $g(u, v)$  are the reaction terms that determine the dynamics of the system;  $0 < a < 1/2$ ,  $b \geq 0$  and  $\gamma \geq 0$  are three key parameters; and  $\nabla^2$  is the Laplacian Operator. The term  $\nabla^2 u$  is associated with the diffusion characteristics. Recently, Zhao [Zhao et al., 2010] presented a revised or R-FHN model to describe the behaviour of wave formation in a BZ reaction that is identifiable directly from experimental data by introducing a diffusion term  $D_v(k)\nabla^2 v$  for the variable  $v$ . The diffusion coefficient  $D_v(k)$ , a function of the curvature of the wavefront, can be identified from the propagation speed. The parameter  $\gamma$  is determined from the profile of the steady state wave and  $a, b$  are chosen to achieve the steady wave.

It has been observed that in a BZ reaction oscillating waves always arise even without manual interference. Both the traditional FHN model and the revised or R-FHN model can describe only one travelling wave. It is therefore important to seek a model that can describe not only propagation characteristics for a single wave but also for oscillating waves. To solve this problem, this paper introduces a new Temperature Dependent or TD-FHN model that is given by

$$\begin{aligned}\frac{\partial u}{\partial t} &= u(a - u)(u - 1) - v + D_u(T)\nabla^2 u \\ \frac{\partial v}{\partial t} &= b(T)u - \gamma v + D_v\nabla^2 u\end{aligned}\tag{2}$$

where  $T$  is the reaction temperature which influences the diffusion coefficient  $D_u$  and the parameter  $b$ . The method to determine  $\gamma$  is the same as described in the R-FHN model. Based on different temperatures, to determine the other four parameters  $a, b, D_v, D_u$ , two characteristics of the wave formation are considered in this paper: the oscillation frequency and propagation speed.

### 2.1 Chemical Oscillation Behaviours

A wave that represents an excursion from a steady state and back to it, will be called a pulse wave and can be excited if a certain threshold perturbation is exceeded. Figure

1.(a) shows the phase portrait of a typical wave produced by a traditional FHN model. Starting from an initial value  $(u_0, v_0) = (0.2, 0)$ , denoted by  $A$  in Figure 1.(a), the trajectory of  $(u, v)$  follows the curve in the sequence  $A \rightarrow B \rightarrow C \rightarrow D \rightarrow E$  until it reaches the steady state  $(u_s, v_s) = (0, 0)$ . To excite such a wave, the initial values must be larger than a threshold, or  $(u, v)$  reverses back to the steady state very quickly. The temporal evolution of the variables  $u$  and  $v$  of the excited wave are illustrated by Figure 1.(b) and (c) respectively. There are two factors that determine if the model

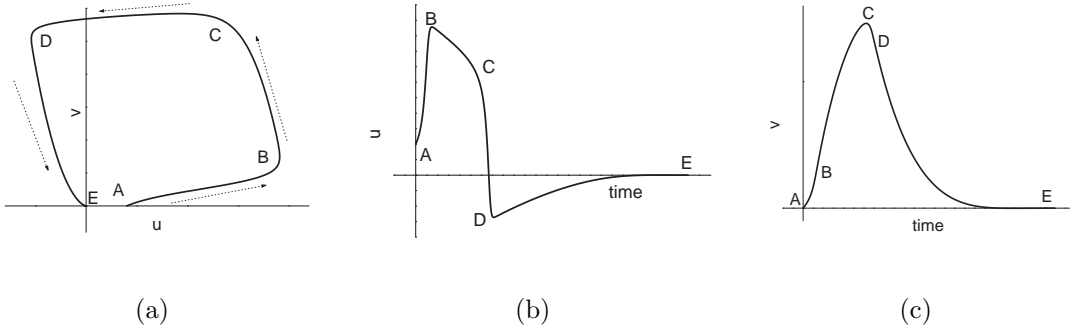


Figure 1: (a) Phase portrait of a wave for a FHN model with  $a = 0.1, b = 0.005, \gamma = 0.016$  with the initial values  $(u_0, v_0) = (0.2, 0)$ ; (b) Temporal evolution of  $u$  corresponding to the phase-space behaviour in (a); (c) Temporal evolution of  $v$  corresponding to the phase-space behaviour in (a).

can exhibit oscillation behaviour: the steady states, and the trajectory contour of  $(u, v)$ . The condition to generate an oscillation is to keep the trajectory contour away from the steady states as far as possible.

The null clines for the two variables  $u, v$  can be written as:

$$\begin{aligned} f(u, v) &= u(a - u)(u - 1) - v = 0 \\ g(u, v) &= bu - \gamma v = 0 \end{aligned} \quad (3)$$

The steady states can be determined by solving the equation

$$u(a - u)(u - 1) = \frac{b}{\gamma}u \quad (4)$$

Since Eq. (4) is a cubic equation, it can have either one or three real solutions. Hence, the number of steady states is only determined by  $a$  and  $\frac{b}{\gamma}$ .

Because the parameters  $b$  and  $\gamma$  are much less than  $a$ , the variable  $u$  changes much faster than  $v$ . Thus, the trajectory contour of  $(u, v)$  mainly depends on the curve  $f(u, v) = 0$ , where  $a$  is the only parameter. There are three solutions for  $f(u, v) = 0$  when  $v = 0$ :

$u = 0, u = a$  and  $u = 1$ . In the traditional FHN model,  $a$  is set between zero and 0.5. Figure 2.(a) shows the null clines for  $u, v$  when  $a = 0.1$ , where the model obviously has only one steady state  $(u_s, v_s) = (0, 0)$ . The trajectory contour of the final stage follows  $f(u, v) = 0$  and eventually enters the steady state, as illustrated by the red curve. Thus the system is monostable. If  $\frac{b}{\gamma}$  is decreased, there may be three steady states, as shown in Figure 2.(b). The trajectory contour may eventually enter the steady state  $S_3$  or the steady state  $S_1$  depending on the initial values, as illustrated by the red curves. Thus, the system is bistable. The above results are also applicable for the case when  $a = 0$ .

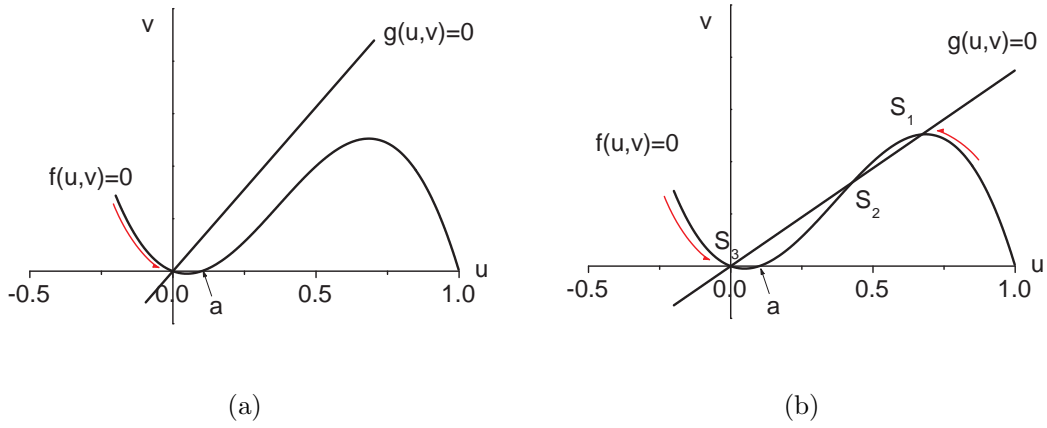


Figure 2: (a) Null clines for  $u, v$  when  $a = 0.1$  and  $\frac{b}{\gamma}$  is chosen to produce one steady states; (b) Null clines for  $u, v$  when  $a = 0.1$  and  $\frac{b}{\gamma}$  is chosen to produce three steady states.

Hence, it is impossible to exhibit oscillatory behaviours if  $a \geq 0$  no matter how many steady states the model has.

If  $a < 0$  and there is only one steady state, as shown in Figure 3.(a). Starting from the point A, the system moves slowly along the null cline as  $v$  decreases from A to B. Upon reaching B,  $u$  will rapidly increase as the system jumps to the other branch of the  $f(u, v) = 0$  null cline (C). This branch is in the positive region of  $g(u, v)$ , so the system will move along the  $u$ -null cline towards D as  $v$  slowly increases. Upon reaching D, the system again jumps to the other branch of the  $u$ -null cline and makes a rapid transition to E. It then proceeds back towards to A, and the oscillation occurs. If  $a$  is decreased and  $\frac{b}{\gamma}$  is fixed, there may be three steady states, as illustrated by Figure 3.(b). The trajectory contour may enter into the steady state  $S_1$  or  $S_3$ , which means that the system is bistable. Hence if  $\frac{b}{\gamma}$  is fixed, to exhibit oscillatory behaviours, the parameter

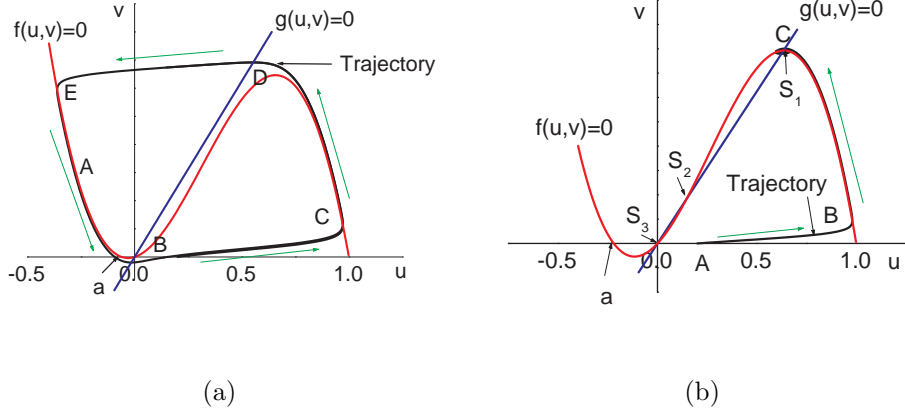


Figure 3: (a) Null clines for  $u, v$  of the model that has one steady state and corresponding phase portrait when  $a = -0.06, b = 0.005, \gamma = 0.016$  with the initial values  $(u_0, v_0) = (0.2, 0)$ ; (b) Null clines for  $u, v$  of the model that has three steady states and corresponding phase portrait when  $a = -0.220, b = 0.005, \gamma = 0.016$  with the initial values  $(u_0, v_0) = (0.2, 0)$ .

$a$  in the TD-FHN model must satisfy

$$a_2 < a < a_1 < 0 \quad (5)$$

Note, if  $a < 0$  but is very close to zero, the trajectory contour may be too close to the steady state to exhibit the oscillation, which is the reason to introduce  $a_1$ . The values of  $a_1, a_2$  depend on the value of  $\frac{b}{\gamma}$ . Figure 4 summarizes the distribution of the three major regions based on different values of the parameters. The blue curve is determined by the number of solutions for Eq. (4).

It is well known that the chemical oscillation frequency in BZ reactions changes under different temperatures. It is therefore important to investigate how to control the frequency of oscillations using the parameters in the Temperature Dependent or TD-FHN model. As the parameter  $\gamma$  can be determined by the profile of the wave, this paper studies the dependence of the oscillation frequency on  $a$  and  $b$ . Figure 5.(a) shows a 3D surface of oscillation frequency for different values of  $a$  and  $b$ . Note the selection of  $a$  has to be limited between  $a_1$  and  $a_2$  along with all tested values of  $b$  to generate valid oscillatory waves. Inspection of the surface shows that both parameters have influence on the oscillatory frequency, but  $b$  plays a more important role than  $a$ . Moreover, to generate oscillation behaviours, the range of selection of  $a$  is very limited, which means that the rate of the maximum and the minimum frequency that this model can produce

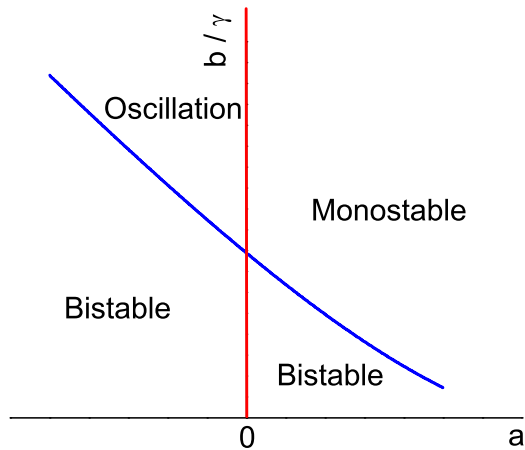


Figure 4: Distribution of stability for the FHN model. Shown here are three major regions of stability under different values of  $a$  and  $\frac{b}{\gamma}$ .

is relatively small if  $a$  is chosen as the control variable. In this paper,  $b$  will therefore be chosen as the variable to control the frequency. Once the dependence of  $b$  on the frequency is established, it is straightforward to identify the function  $b(T)$  directly from the experimental data by utilizing the dependence of chemical frequency on the temperature. Figure 6 shows three snapshots of the temporal evolution of the variable  $v$  with different values of  $b$  and fixed  $a$  and  $\gamma$ . Figure 5.(b) shows that  $b$  as a function of frequency when

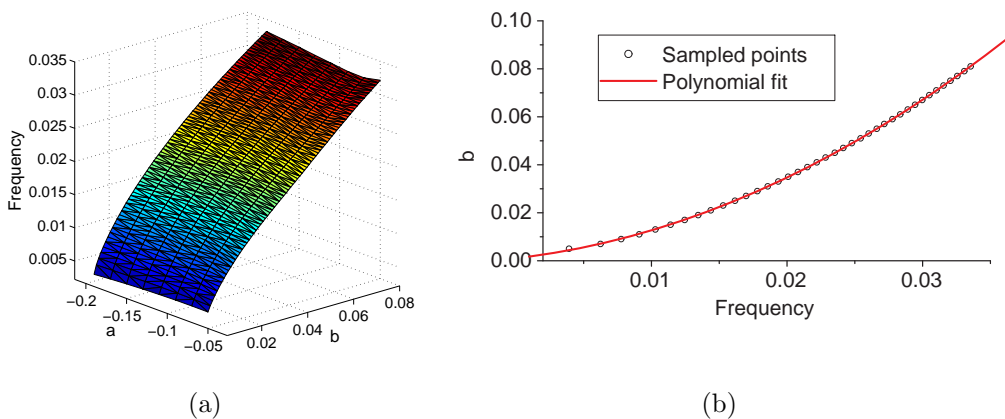


Figure 5: (a) Dependence of the oscillatory frequency on the parameter  $b$  and  $a$ ; (b) Dependence of the oscillatory frequency on  $b$  when  $a = -0.2$  and the estimated polynomial model fit.

$a = -0.2$  and also shows that a second order polynomial model produced an excellent

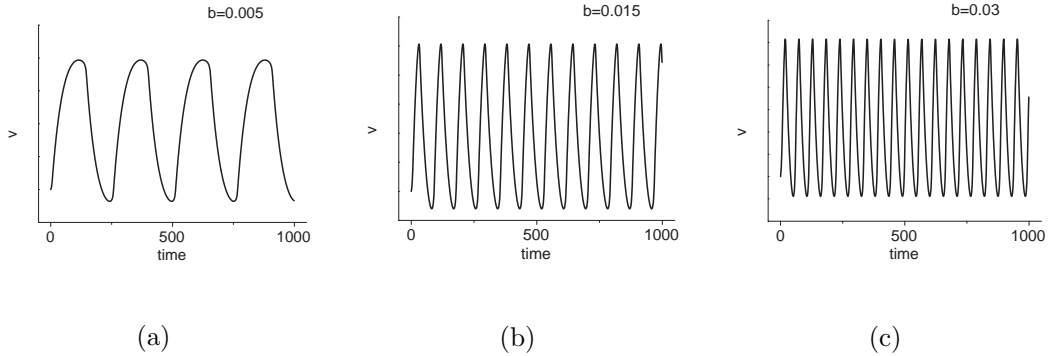


Figure 6: Temporal evolution of  $v$  based on different values of  $b$  with  $a = -0.2$  and  $\gamma = 0.016$ . (a)  $b = 0.005$ ; (b)  $b = 0.015$ ; (c)  $b = 0.03$ .

fit to this relationship. The polynomial model is given by

$$b = 0.001 + 0.6442f_s + 51.903f_s^2 \quad (6)$$

where  $f_s$  denotes the oscillation frequency generated by the TD-FHN model.

## 2.2 Propagation Speed

Propagation speed of a diffusion field is one of the most important characteristics of a reaction-diffusion system, and has been widely used to study the propagation behaviour of BZ reactions [Aliev, 1994]. In the R-FHN model, an extra term  $D_v \nabla^2 v$  was introduced to control the propagation speed, where  $D_v$  is a function of  $k$ , the curvature of the wavefront. It has been observed that compared with the average speed, the offset of the speed contributed by the variety of curvatures is relatively small. Hence, in this paper, the propagation speed is assumed to be a function of temperature  $T$  only.

Zhao [Zhao et al., 2010] observed that at room temperature, the ratio of the maximum and the minimum propagation speed for the BZ reaction is only 1.26. This can be accommodated by the R-FHN model which can have a ratio of 1.46. However, because the experimental temperature of the BZ reactions discussed in this paper was changed in the range from  $15^\circ C$  to  $45^\circ C$ , a significant difference in the propagation speed has been observed where the max-min ratio can reach up to 4, which indicates the method of using  $D_v$  to control the propagation speed is not appropriate in this particular case. To overcome this problem, the TD-FHN model introduced in this paper uses the diffusion

term associated with the variable  $u$  with a variable diffusion coefficient  $D_u(T)$  to control the propagation speed, and  $D_v$  is set to zero. Simulation results suggest this method can provide a wider range of propagation speeds.

Now consider the dependence of the propagation speed  $c_s$  of the simulation model on the parameters  $b$  and  $D_u$ . Assume  $a = -0.2, \gamma = 0.016, D_u = 1$ . By varying the values of  $b$ , the dependence of the propagation speed on the  $b$  can be illustrated in Figure 7.(a). A linear model was fitted to describe the relationship between  $b$  and  $c$  and is written as:

$$c_s = 0.9893 - 4.4405b \quad (7)$$

Assume  $a = -0.2, \gamma = 0.016, b = 0.005$ . By varying the values of  $D_u$ , the dependence of the propagation speed on the  $D_u$  can be illustrated by Figure 7.(b). A second order polynomial model was fitted to describe the relationship between  $D_u$  and  $c$  and is written as:

$$c_s = 0.3012 + 0.7392D_u - 0.0994D_u^2 \quad (8)$$

or

$$D_u = -0.0062 - 0.0109c_s + 1.1092c_s^2 \quad (9)$$

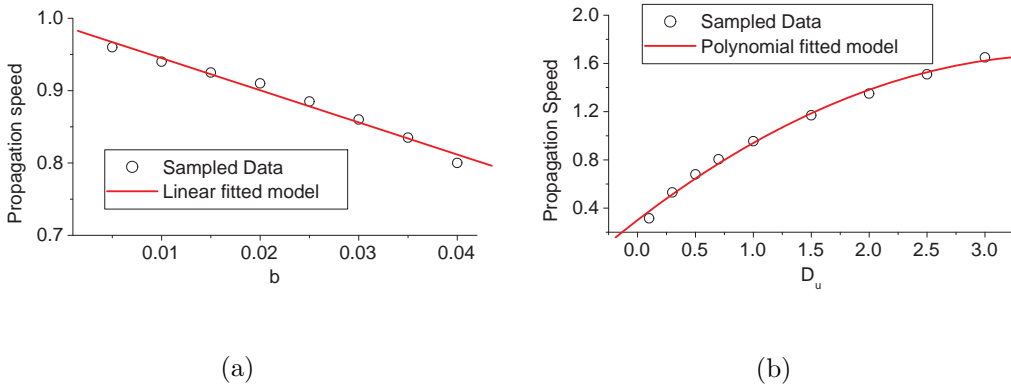


Figure 7: (a) Dependence of the propagation speed  $c_s$  on the  $b$  for the TD-FHN model when  $a = -0.2, \gamma = 0.016, D_u = 1$ ; (b) Dependence of the propagation speed  $c_s$  on the  $D_u$  for the TD-FHN model when  $a = -0.2, \gamma = 0.016, b = 0.005$ .

If  $D_u$  is changed from 0.1 to 3, Eq. (8) shows that the ratio of maximum speed and minimum speed contributed by  $D_u$  can reach up to 4.81, which is sufficiently wide to cover the speed range of the real data. As the parameter  $b$  has been used to control the oscillation frequency, its influence on the propagation speed is inevitable. Hence,

to accurately control the speed using  $D_u$ , the contribution of speed from  $b$  must be considered.

### 3 Identification from BZ Experimental Data

The apparatus set-up used for the temperature controlled BZ reactions is illustrated in Figure 8. The chemical processor was prepared in a thin layer, the temperature was controlled by a thermostatic water circulator, and the recipe was adapted from [Winfree, 1972]. Before dropping the mixed solution in the dish, 15 minutes was allowed so that the dish can reach the designed temperature as close as possible. Before the experiment was commenced, a thermometer was employed to measure the difference between the actual temperature of the dish surface and the designed temperature in the thermostatic water circulator because the dish was open to the air. It has been observed that there is a  $4 - 5^\circ C$  difference between them. All values of temperature discussed in this paper relate to the actual temperatures of the solution. The data were acquired using a CCD camera with a resolution of  $768 \times 576$  pixels in 24 bit true color levels. The sample rate was chosen as 5 frames per second (fps) controlled by a computer. A typical image represents an area of size  $69.12mm \times 51.84mm$  with a resolution of  $0.09mm$  per pixel. For one group of data, starting right after the first excitation was observed, about 200 seconds of data were recorded to capture the initial excitation stage and the subsequent oscillation behaviour. Six different temperatures ( $15^\circ C, 20^\circ C, 25^\circ C, 30^\circ C, 35^\circ C, 45^\circ C$ ) were implemented and the experiments for each temperature were repeated three times. The blue component of a pixel, which always has better performance in distinguishing the wavefront and the background compared with the green and red components for the BZ reaction, was extracted from the raw images to describe the waves.

Before identification, it is important to define the spatio and temporal calibrations, which is crucial to generate a model with physical meaning. Assume  $t_s$  is the time in the simulation model,  $t_r$  is the time in the real world;  $d_s$  is the spatial unit in the simulation model and  $d_r$  is the spatial unit in the real world. The coefficient of the temporal calibration  $k_t$  and the coefficient of the spatial calibration  $k_d$  can be written as

$$\begin{aligned} k_t &= t_s/t_r \\ k_d &= d_s/d_r \end{aligned} \tag{10}$$

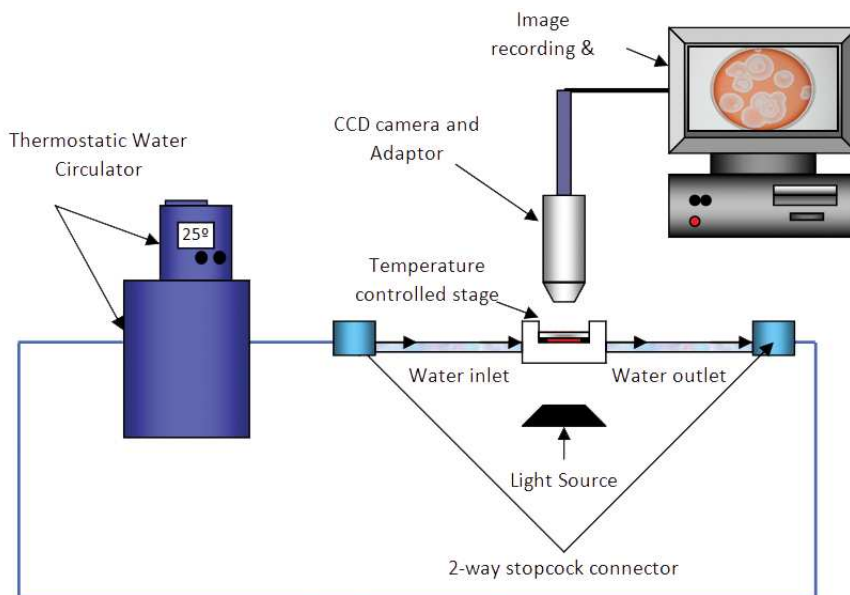


Figure 8: Schematic representation of experimental set-up used in the temperature controlled BZ reaction.

The determination of the unknown parameters based on the observations will be considered in the following sections.

### 3.1 Chemical Oscillation Frequency

To generate a temporal evolution graph for a considered position  $(x_p, y_p)$  in the image, the values of the blue component for all acquired sequential images of a group in that position were recorded. Figure 9.(a)-(f) show six graphs of temporal evolution of experimental data for each tested temperature. The oscillation frequency for the waves, denoted by  $f_r$ , was calculated by counting the number of valid waves during a fixed time interval. The measured frequencies were averaged by processing three groups of data under each temperature, and the results are shown in the second row of Table 1 and also illustrated by Figure 10, which clearly indicates the frequency is nonlinear in temperature. To quantitatively establish the relationship between temperature and frequency, an exponential model was fitted and is written as:

$$f_r = 0.006e^{T/14.0894} \quad (11)$$

Note the sampled temperatures were limited within  $15^\circ$  and  $45^\circ$ . Equation (11) has not been tested outside of this range.

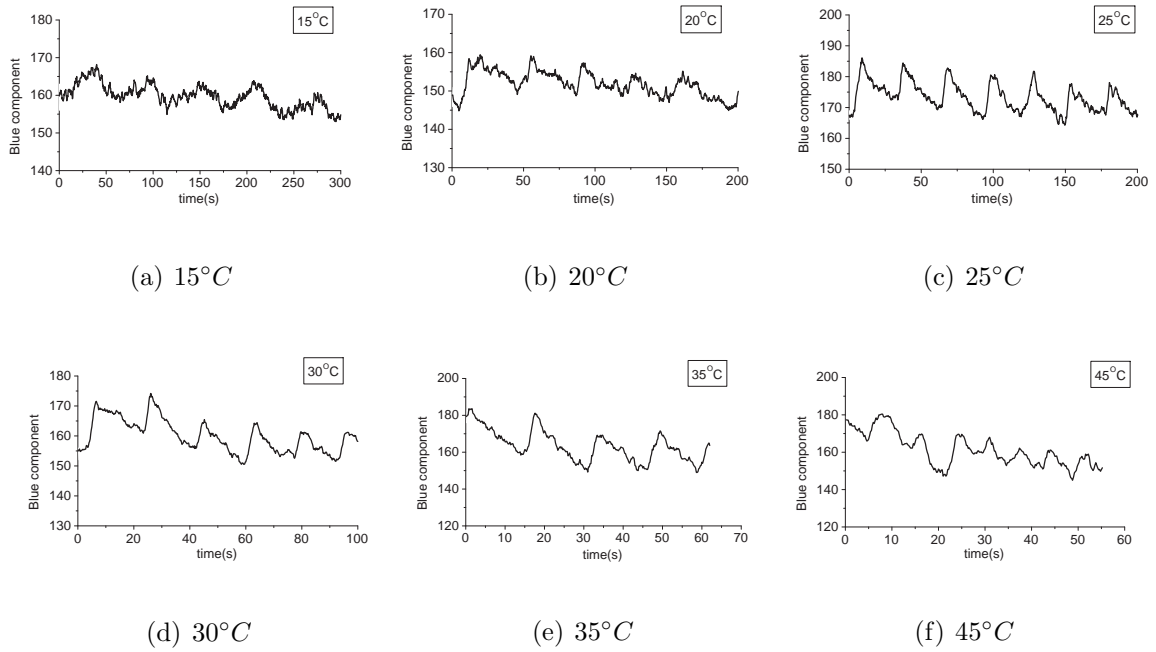


Figure 9: Six temporal evolutions for a considered position  $(x_p, y_p)$  of the BZ reactions under different temperatures.

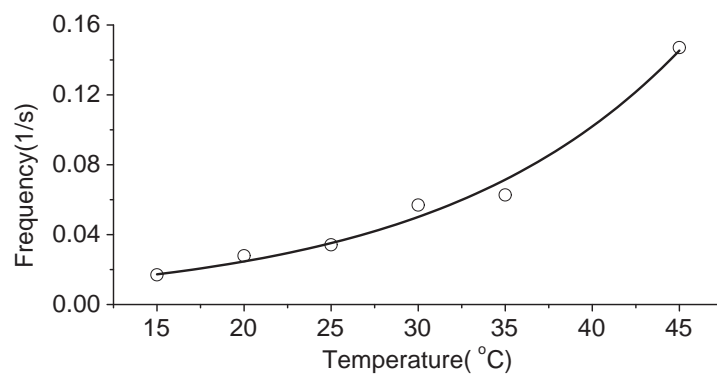


Figure 10: Measured frequencies for different temperatures and corresponding exponential fitting.

The coefficient of temporal calibration  $k_t$  must be determined before establishing the relationship between temperature and the parameter  $b$ . Consider

$$\frac{f_r}{f_s} = k_t \quad (12)$$

where  $f_r$  denotes the oscillatory frequency in the real world and  $f_s$  denotes the oscillatory frequency in the simulation model. Figure 5.(b) shows that  $f_s$  is typically located between  $0.05 \sim 0.032$  and Table 1 shows the frequency from the real data lies between  $0.02Hz \sim 0.16Hz$ . Hence, for this example,  $k_t$  is set as 5. The parameter  $b$  can finally be written as a function of temperature  $T$  by substituting Eq. (11) into Eq. (6), to given

$$b(T) = 0.001 + 7.7304 \times 10^{-4} e^{T/14.0894} + 7.474 \times 10^{-5} e^{T/7.0447} \quad (13)$$

The third row of Table 1 shows the corresponding estimated values of  $b$  for different temperatures using Eq. (13).

Table 1: Measured oscillation frequencies and corresponding estimated values of  $b$  for different temperatures

$T(^{\circ}C)$	Measured $f_r$ (hz)	$b$
15	0.01698	0.00387
20	0.02789	0.00547
25	0.03419	0.00816
30	0.05695	0.01278
35	0.06270	0.02102
45	0.14706	0.06428

### 3.2 Propagation Speed

The propagation speed was measured for each group of data and was averaged for each group under the same temperature. The results are shown in the second row of Table 2, which clearly shows that the speed increases following an increment in temperature. Before identification, the coefficient of spatio calibration  $k_d$  must be determined. Based on Eq. (10), the relationship between the propagation speed in the real world ( $c_r$ ) and in the simulation model ( $c_m$ ) is given by

$$c_s = \frac{k_d}{k_t} c_r \quad (14)$$

Inspection of the second row of Table 2 shows that the real propagation speed is limited to be between  $[0.06866\text{mm/s}, 0.26091\text{mm/s}]$ . In this paper  $k_d$  will therefore be chosen as 25, which indicates that the range of the propagation speed required for the TD-FHN model should be in the range of  $[0.3433, 1.30455]$  which is within the working range of the proposed model, as shown in Figure 7.(b).

The next objective is to determine  $D_u(T)$  based on the above results. Assuming  $b = 0.005$  as the reference, the offset of propagation speed contributed by  $b$  can be calculated based on Eq. (7) and the results are shown in the third row of Table 2. The values of  $D_u$  can then be estimated from Eq. (9), and the results are shown in the fourth row of Table 2. The dependence of  $D_u$  on the temperature is illustrated by in 11, where a second order

Table 2: Measured propagation speeds, speed offset contributed by  $b$  and corresponding estimated values of  $D_u$  for different temperatures from experimental data

$T(^{\circ}C)$	Detected Speed $c_r(\text{mm/s})$	Speed Offset from $b$	Estimated $D_u$
15	0.06866	0.00100	0.11705
20	0.10450	-0.00042	0.29335
25	0.14353	-0.00281	0.57966
30	0.20238	-0.00691	1.19706
35	0.23634	-0.01423	1.72109
45	0.26091	-0.05264	2.70313

polynomial model was fitted and can be expressed as

$$D_u(T) = -0.52292 + 0.0212T + 0.00115T^2 \quad (15)$$

### 3.3 Model Validation

By analysing the characteristics of the oscillatory frequency and propagation speed of the BZ reaction, the dependence of  $b$  and  $D_u$  in the proposed TD-FHN model have been identified using two polynomial models. Combining all the previous results the identified

TD-FHN model can finally be described as

$$\begin{aligned}
\frac{\partial u}{\partial t} &= u(a - u)(u - 1) - v + D_u(T)\nabla^2 u \\
\frac{\partial v}{\partial t} &= b(T)u - \gamma v \\
b(T) &= 0.001 + 7.7304 \times 10^{-4}e^{T/14.0894} + 7.474 \times 10^{-5}e^{T/7.0447} \\
D_u(T) &= -0.52292 + 0.0212T + 0.00115T^2
\end{aligned} \tag{16}$$

where  $15 \leq T \leq 45$ ,  $a = -0.2$  and  $\gamma = 0.016$ .

To validate the model, the oscillation frequency and propagation speed were reconstructed using Eq. (16) and the results are shown in Figure 12, which clearly shows the identified model has captured the key properties of the BZ reaction under controlled temperatures.

## 4 Conclusions

System identification of excitable media is a potentially important tool for unravelling the complex relationships between the observed patterns and the system control variables. This paper has introduced for the first time a method for the identification of a Temperature Dependent or TD-FHN model for the oscillatory waves of experimentally observed BZ reactions directly from time lapse imaging data. An important contribution of the paper, has been to embed a physical variable into a purely mathematical model,

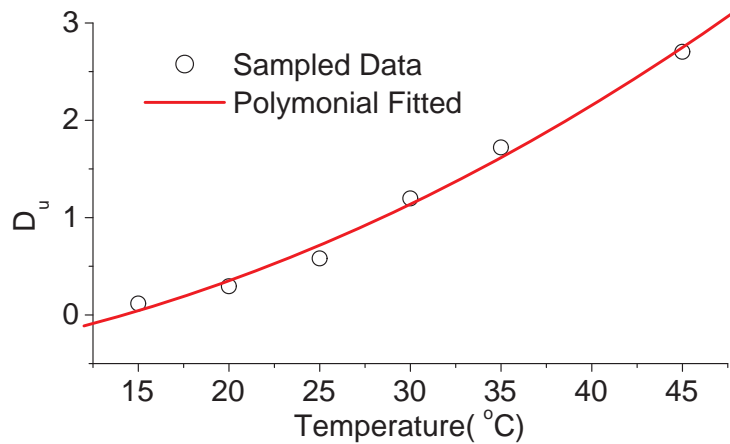


Figure 11: Dependence of  $D_u$  on the temperature of the BZ reaction and corresponding polynomial fitting.

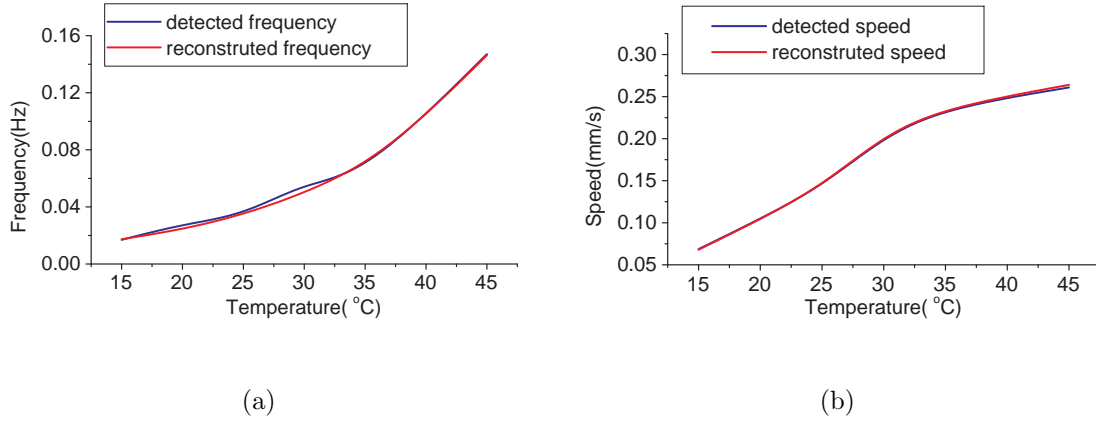


Figure 12: (a) Comparison of the reconstructed and measured oscillation frequency over temperature; (b) Comparison of the reconstructed and measured propagation speed over temperature.

which opens the way to identify the widely used simulation models for reaction-diffusion systems from experimental observations with controlled inputs.

Initially, the method to generate oscillatory waves was proposed along with the corresponding stability analysis. With different values of the parameters, the system can be either monostable, oscillatory, or bistable. By studying the dynamics of the oscillation frequency and propagation speed under different temperatures, two key parameters  $b$  and  $D_u$  were identified as functions of the temperature. Finally, a TD-FHN model expressed as Eq. (16) has been produced to describe the dynamics of propagating oscillating waves in a BZ reaction under controlled temperature experiments. Results of the validation show that the curves of the reconstructed dependence of frequency and speed on the temperature are very close to the measured data, which indicates the method proposed in this paper is highly encouraging.

## Acknowledgment

The authors gratefully acknowledge that part of this work was financed by Engineering and Physical Sciences Research Council (EPSRC), UK, and by the European Research Council (ERC).

## References

- A. Adamatzkya, B. L. Costello, C. Melhuisha, and N. Ratcliffe. Experimental implementation of mobile robot taxis with onboard belousov-zhabotinsky chemical medium. *Materials Science and Engineering C*, 24(4), 2004.
- R. R. Aliev. Oscillation phase dynamics in the belousov-zhabotinsky reaction - implementation to image-processing. *Journal Of Physical Chemistry*, 95(15):3999–4002, 1994.
- T. Bansagi, M. Leda, M. Toiya, A. M. Zhabotinsky, and R. Epstein I. High-frequency oscillations in the belousov-zhabotinsky reaction. *The Journal of Physical Chemistry A*, 113:5644–5648, 2009.
- M. H. Chou, H. C. Wei, and Y. T. Lin. Oregonator-based simulation of the belousov-zhabotinskii reaction. *International Journal of Bifurcation and Chaos*, 17(12):4337–4353, 2007.
- R. Field and R. Noyes. Oscillations in chemical systems iv. limit cycle behavior in a model of a real chemical reaction. *Journal of Chemical Physics*, 60:1877–1884, 1974.
- R. FitzHugh. Mathematical models of threshold phenomena in the nerve membrane. *Bulletin of Mathematical Biology*, 17(4):257–278, 1955.
- P. Glansdorff and I. Prigogine. *Thermodynamic Theory of Structure, Stability and Fluctuations*. Wiley Interscience, New York, 1971.
- P. Gray and S. K. Scott. Autocatalytic reactions in the isothermal continuous stirred tank reactor: isolas and other forms of multistability. *Chemical Engineering Science*, 38(1):29–43, 1983.
- Y. Guo, Y. Zhao, S.A. Billings, D Coca, R. I. Ristic, and L DeMatos. Identification of excitable media using a scalar coupled mapped lattice model. *International Journal of Bifurcation and Chaos*, 20(7):2137–2150, 2010.
- Y. Ito, M. Nogawa, and R. Yoshida. Temperature control of the belousov-zhabotinsky reaction using a thermoresponsive polymer. *LANGMUIR*, 19(23), 2003.

- A. Kaminaga, K. V. Vladimir, and R. E. Irving. A reaction-diffusion memory device. *Angewandte Chemie International Edition*, 45(19), 2006.
- E. Koros. Monomolecular treatment of chemical oscillation. *Nature*, 251:703–704, 1974.
- S. R. Pullela, D. Cristancho, P. He, D. W. Luo, K. R. Hall, and Z. D. Cheng. Temperature dependence of the oregonator model for the belousov-zhabotinsky reaction. *Physical Chemistry Chemical Physics*, 11(21):4236–4243, 2009.
- V. K. Vanag and I. R. Epstein. Design and control of patterns in reaction-diffusion systems. *Chaos*, 18(2), 2008.
- A. T. Winfree. Spiral waves of chemical activity. *Science*, 175:634–636, 1972.
- A. M. Zhabotinskii. Periodical oxidation of malonic acid in solution. *Biofizika*, 9: 306–311, 1964.
- Y. Zhao, S. A. Billings, and A. F. Routh. Identification of the belousov-zhabotinskii reaction using cellular automata models. *International Journal of Bifurcation and Chaos*, 15(5):1687–1701, 2007.
- Y. Zhao, S.A. Billings, Y. Guo, D. Coca, R. I. Ristic, and L. DeMatos. Spatio-temporal modelling of wave formation in an excitable chemical medium based on a revised fitzhugh-nagumo model. *International Journal of Bifurcation and Chaos*, 2010. (to appear).